

PHOTODESORPTION FROM ICES CONTAINING H₂CO AND CH₃OH

G. Féraud¹, M. Bertin¹, C. Romanzin², R. Dupuy¹, F. Le Petit¹, E. Roueff¹, L. Philippe¹, X. Michaut¹, P. Jeseck¹ and J.-H. Fillion¹

Abstract. The interplay between gas and ice is expected to play an important role in the observed molecular abundances in cold and dense regions of the interstellar medium (ISM). The role of non-thermal desorption from grains in the origin of the gaseous organic molecules observed in these regions is still an open question. UV photodesorption from icy grains containing formaldehyde (H₂CO) and methanol (CH₃OH) has been invoked as a possible non-thermal mechanism that participates to the observed gas phase H₂CO and CH₃OH abundance.

We studied the photon-induced desorption from H₂CO and CH₃OH-containing ices in the Far-UltraViolet (FUV) range at the SOLEIL synchrotron (DESIRS beamline, 7-13.6 eV, 910-1771 Å), and we detected the gas phase release of intact H₂CO and of intact CH₃OH, but also of photofragments as a function of the photon energy. The photodesorption of intact H₂CO from pure H₂CO ice is higher than the CH₃OH average photodesorption yield from pure CH₃OH ice. In more astrophysically-relevant H₂CO:CO ice mixtures, the photodesorption of H₂CO seems to be enhanced by the presence of CO, whereas on the contrary, the photodesorption of CH₃OH is reduced in CH₃OH:CO mixtures. This shows the ability of UV photons to desorb small organic molecules, such as H₂CO.

Keywords: gas-to-ice ratio, photodesorption, photodissociation, condensed phase, protoplanetary disks (PPD), photon dominated regions (PDR), Complex Organic Molecules (COMs)

1 Introduction

In the Interstellar Medium (ISM), icy grain mantles are mainly composed of H₂O and CO, but also of larger organic molecules such as methanol (CH₃OH), and certainly also formaldehyde (H₂CO). CH₃OH is one of the most basic Complex Organic Molecules (COMs), while H₂CO is a COM precursor. It is proposed that H₂CO and CH₃OH can both be formed on grains through the successive hydrogenation of CO. H₂CO can also be formed directly in the gas phase, but CH₃OH cannot and therefore its presence in the gas phase can only be explained by non-thermal desorption from icy grains.

Gas phase CH₃OH and H₂CO are observed in various regions, such as prestellar cores (Bacmann et al. 2003; Vastel et al. 2014), photon dominated regions (PDR) (Guzmán et al. 2011, 2013) and protoplanetary disks (PPD) (Walsh et al. 2016; Carney et al. 2019). In many cases, observations together with astrochemical modelling suggest that non-thermal desorption mechanisms must be at play to explain their gas phase abundances. Very recently, the desorption of intact CH₃OH by swift heavy ions, analogs of cosmic-rays, has been shown to be a dominant process in dense clouds (Dartois et al. 2019). UV photodesorption, where UV photons are responsible for the desorption of molecules lying in the upper layers of the icy grains, is another non-thermal mechanism, and its importance in PDR and PPD has been highlighted (eg Guzmán et al. (2011); Walsh et al. (2017)). Whereas photodesorption studies have been mostly focused on small molecules (CO, N₂, CO₂, H₂O; eg Öberg et al. (2009); Fayolle et al. (2011); Bertin et al. (2013); Fillion et al. (2014); Cruz-Diaz et al. (2018)), it is much less known for larger organic molecules. Measurements of photodesorption yields are however crucial, as their variations could increase gas phase abundances by up to several orders of magnitude in some environments, (Guzmán et al. 2011) but also induce changes in the solid-phase chemistry (Esplugues et al. 2016, 2017) and possibly in the gas phase chemistry, and even in the location of snowlines. There is thus a strong need for laboratory astrophysics

¹ Sorbonne Université, Observatoire de Paris, Université PSL, CNRS, LERMA, F-75005, Paris, France

² Laboratoire de Chimie Physique (LCP), CNRS UMR 8000, Univ. Paris Sud, F-91400 Orsay, France

studies to understand photodesorption mechanisms and obtain quantified data for astrophysically-relevant ices containing organic molecules. This is what is presented here, for pure H_2CO and CH_3OH ices, and for H_2CO or CH_3OH mixed with CO .

2 Experimental results

The SPICES (Surface Processes & ICES) set-up was used for these experiments. It consists in an ultrahigh vacuum (UHV) chamber within which a polycrystalline gold surface is cooled down to ~ 10 K. H_2CO and CH_3OH ices of controlled thicknesses are grown on this gold surface (see Bertin et al. (2016); Féraud et al. (2019) for experimental details), either as pure ices or mixed with CO ($\text{H}_2\text{CO}:\text{CO}$ and $\text{CH}_3\text{OH}:\text{CO}$). Several diagnostics are possible in this setup, both regarding gas and solid phase. In this proceeding, we focus on the detection of gas phase molecules released from the ices irradiated with photons, i.e. photodesorbing neutral molecules, with a quadrupole mass spectrometer (QMS, from Balzers).

The chamber was coupled to the undulator-based DESIRS beamline (Nahon et al. 2012) at the SOLEIL synchrotron facility, which provides monochromatic, tunable VUV light for irradiation of our ice samples. To acquire H_2CO photodesorption spectra, the narrow bandwidth (~ 25 meV) output of a grating monochromator is continuously scanned between 7 and 13.6 eV. For CH_3OH , the photodesorbing signal is close to the detection limit. Thus higher photon flux irradiation conditions, using lower resolution (0.5 eV) by sending directly the output of the undulator, are preferred in this case. The photodesorption of molecules in the gas phase following VUV irradiation of the ices monitored with the QMS is then converted into an absolute photodesorption yield, in molecule per incident photon (Dupuy et al. 2017a).

2.1 Pure H_2CO and Pure CH_3OH ices

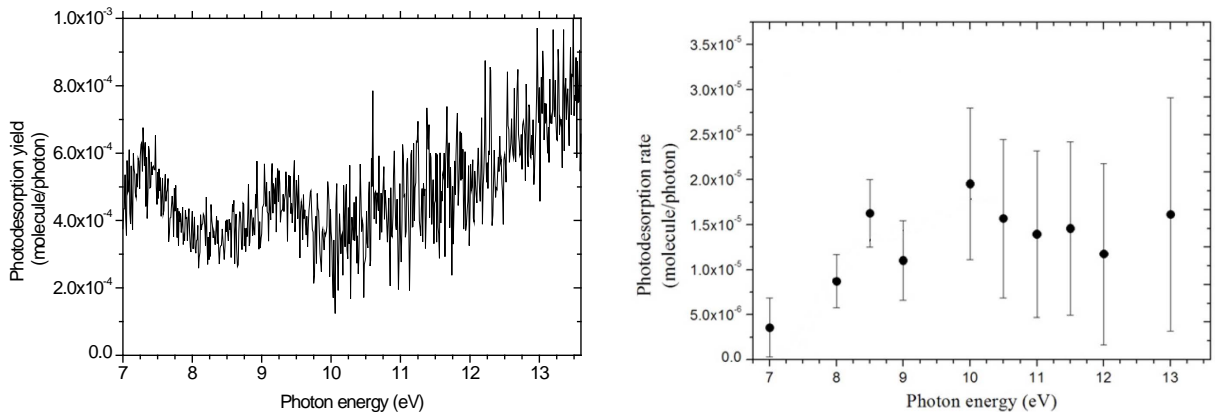


Fig. 1. **Left:** Absolute H_2CO photodesorption spectrum from a 15 ML thick H_2CO ice on gold at 10 K between 7 and 13.6 eV from Féraud et al. (2019). **Right:** Absolute CH_3OH photodesorption spectrum from a 20 ML thick CH_3OH ice on gold at 10 K between 7 and 13 eV from Bertin et al. (2016).

Photodesorption spectra, representing the absolute photodesorption yield, in molecule per incident photon, as a function of the photon energy, are represented in Figure 1, from Bertin et al. (2016) and Féraud et al. (2019). We notice that H_2CO photodesorption from H_2CO ice is more efficient than CH_3OH desorption from CH_3OH ice. This strengthens the fact that photodesorption yields span over orders of magnitude for different ice constituents : it is $\sim 5 \times 10^{-4}$ molecules/photon for H_2CO , $\sim 10^{-5}$ molecules/photon for CH_3OH , whereas it is $\sim 10^{-2}$ molecules/photon for CO (Fayolle et al. 2011).

Regarding the shape of the spectrum, the CH_3OH one follows the absorption spectrum from Cruz-Diaz et al. (2014) in the low energy range (cf Bertin et al. (2016)), meaning that the electronic excitation of CH_3OH is the first step prior to desorption. For H_2CO , such a comparison between absorption and photodesorption cannot be done because of the lack of VUV absorption spectrum of solid H_2CO . There are elements pointing towards the dissociative nature of the H_2CO electronic states seen at ~ 7 eV and ~ 9 eV (cf Féraud et al. (2019)).

Table 1. Average photodesorption yields Y_i ($\times 10^{-4}$ molecule per incident photon; i is the photodesorbed species) for pure H₂CO ice, a mixed H₂CO:CO ice (Féraud et al. 2019), Some photodesorption yields from pure CH₃OH ice and a mixed CH₃OH:CO ice are also reported (the photodesorbing species reported here are not exhaustive, see Bertin et al. (2016) for an exhaustive list), in various interstellar environments with radiation fields from 7 to 13.6 eV

Ice	Photodesorbed species i	ISRF ^a	PDR ^b A _V =1	PDR ^b A _V =5	Secondary UV ^c	Protoplanetary disk TW Hya ^d
($\times 10^{-4}$ molecule/photon)						
Pure H ₂ CO ^e	H ₂ CO	5	4	4	4	4
	CO	45	28	22	45	40
H ₂ CO:CO (1:3) ^e	H ₂ CO	8 [†]	6 [†]	6 [†]	6 [†]	10 [†]
	CO	61	40	38	42	26
Pure CH ₃ OH ^f	CH ₃ OH	0.12			0.15	
	H ₂ CO	0.07			0.12	
CH ₃ OH:CO ^f	CH ₃ OH	< 0.03			< 0.03	
	H ₂ CO	0.07			0.12	

UV fields between 7 and 13.6 eV are taken from : ^a Mathis et al. (1983); ^b PDR Meudon Code Le Petit et al. (2006); ^c Gredel et al. (1987); ^d Heays et al. (2017) (FUV observation of TW-Hydra from France et al. (2014), extrapolated to a broader spectral range); ^e Féraud et al. (2019) ^f Bertin et al. (2016)

[†] This average photodesorption yield is normalized to the fraction of the surface of the ice containing H₂CO f_s (see text for details)

Unravelling the photodesorption mechanisms is an important issue at stake for astrochemical models. For H₂CO, our experiments could not constrain much the possible mechanisms, as four mechanisms could be at play (Féraud et al. 2019) : Desorption induced by electronic transitions in H₂CO (DIET), indirect desorption induced by electronic transitions (for example if the electronic excitation of CO is transferred to H₂CO), kick-out of a H₂CO molecule by an H atom, and reactions between photoproducts HCO + H → H₂CO, or HCO + HCO → H₂CO + CO, leading to the ejection of the newly formed H₂CO. On the other hand, for CH₃OH, reactions between photoproducts were shown to be a major way of releasing CH₃OH in the gas phase (Bertin et al. 2016), through : H₃CO + H → CH₃OH or CH₂OH + H → CH₃OH. This is a good indication that a singular photodesorption mechanism could emerge for specific molecules, such as CH₃OH. Besides, for H₂CO and CH₃OH ices, we observe the photodesorption of fragments (not shown): when irradiating pure H₂CO ices, CO and H₂ fragments desorb (Féraud et al. 2019), whereas when irradiating pure CH₃OH ices, CO, CH₃, OH, H₂CO and H₃CO desorb (Bertin et al. 2016). CO fragments are more abundant when coming from H₂CO ices than from CH₃OH ices (Table 1). This enrichment of the gas phase with photoproducts is an important finding, and it could have various consequences on the gas phase chemistry of the ISM. The importance of photodissociation for organic molecules, whether for solid-to-gas exchanges, or for solid state photochemistry, has thus to be taken into account in astrochemical models.

2.2 Implications for PDR and Protoplanetary Disks

Table 1 reports photodesorption yields for different astrophysical environments, the InterStellar Radiation Field (ISRF), PDR at two different extinctions, A_V=1 and A_V=5, secondary UV generated by H₂ excited by cosmic rays, and the protoplanetary disk TW Hydra (see Dupuy et al. (2017b) for a description of the calculation of photodesorption yields). It should be noted that the experimental CH₃OH photodesorption yield of 10⁻⁵ – 10⁻⁶ molecule/photon (Bertin et al. 2016; Cruz-Diaz et al. 2016) is close to the detection limit of our setup, but it is nevertheless *non negligible* in an astrophysical context, as it is high enough to have an effect on the gas replenishment (Walsh et al. 2017; Ligterink et al. 2018). Photodesorption yields slightly vary from one astrophysical environment to the other (Table 1). However, they depend on the ice composition, as they change if pure or mixed ices are considered. They are slightly larger when H₂CO is mixed with CO, which is an enhancement certainly due to the CO-induced photodesorption of H₂CO. The behaviour is different for CH₃OH ices, as the CH₃OH photodesorption yield is reduced for the CH₃OH ice mixed with CO (Table 1). As a consequence, for the modelisation of an astrophysical ice, yields corresponding to the considered molecule and to the ice composition should be taken from experimental results.

In low-UV illuminated PDR, non-thermal desorption from H₂CO or CH₃OH-containing icy grains is neces-

sary to reproduce the observed abundances, (Guzmán et al. 2011, 2013) and photodesorption was considered to be a very good candidate. The experimental finding that average photodesorption yields are approximately the same at $A_V=1$ and $A_V=5$ implies that for H_2CO , a single photodesorption yield can be used at all extinctions. Experimental photodesorption values can now be used in models, instead of arbitrary ones.

In PPD, models have proposed that photodesorption plays a key role to explain the observations (Walsh et al. 2014, 2016; Carney et al. 2017, 2019). Besides, experimental photodesorption yields of CH_3OH (Bertin et al. 2016; Cruz-Diaz et al. 2016) have triggered modelling refinements and interesting findings related to CH_3OH photodesorption have been found, such as (i) the influence of CH_3OH photodesorption on the abundance of both solid and gas phase CH_3OH by orders of magnitude, in some parts of the disk (Walsh et al. 2017; Ligterink et al. 2018) (ii) The predominance of photodesorption over chemical desorption in the majority of the disk (Ligterink et al. 2018) (iii) The specific shaping of snowlines (Ligterink et al. 2018; Agúndez et al. 2018) (iv) The effect of the desorption of CO fragments from CH_3OH ice on gas phase abundances and on the CH_3OH snowline location (Walsh et al. 2017; Ligterink et al. 2018) (v) Possible dependence of photodesorption on the star properties, that influences gas phase spatial distributions (Walsh et al. 2016; Carney et al. 2019). These conclusions on CH_3OH can directly inspire what could be done with H_2CO , with the recently available experimental photodesorption yields. In addition, detecting CH_3OH in protoplanetary disks is very difficult, so that the best tracer for cold COMs is H_2CO , up to now. However H_2CO has a complicated history, as it could be formed either in the gas phase or in the solid phase. When the release from the solid phase to the gas phase is added, the picture is even more complex. Experimental data such as those reproduced here could thus be used as inputs for models of protoplanetary disks to better constrain the observations.

3 Conclusions

Interstellar H_2CO and CH_3OH are closely intertwined and constitute molecules of wide interest, particularly for their link with COMs. We found that photodesorption from H_2CO - and CH_3OH -containing ices present differences, for example in their yields for pure or CO-mixed ices, but also similarities, as photofragments desorb. These yields and the importance of photofragments should continue to be added in astrochemical models. Based on the example of H_2CO and CH_3OH , it can be proposed that photodesorption from ices containing organic molecules, in the form of the parent molecule or of fragments, certainly plays a role in the physics and chemistry of PPD and PDR. Observational, modelling and laboratory astrophysics efforts have to continue, so that the organic molecules' case keeps clarifying.

The authors thank SOLEIL for provision of synchrotron radiation facilities under the projects 20140100 and 20150760 and also Laurent Nahon and the DESIRS beamline for their help. This work was supported by the Programme National 'Physique et Chimie du Milieu Interstellaire' (PCMI) of CNRS/INSU with INC/INP co-funded by CEA and CNES. Financial support from LabEx MiChem, part of the French state funds managed by the ANR within the investissements d'avenir programme under reference ANR-11-10EX-0004-02, and by the Ile-de-France region DIM ACAV program, is gratefully acknowledged.

References

- Agúndez, M., Roueff, E., Le Petit, F., & Le Bourlot, J. 2018, *Astronomy & Astrophysics*, 616, A19
- Bacmann, A., Lefloch, B., Ceccarelli, C., et al. 2003, *The Astrophysical Journal Letters*, 585, L55
- Bertin, M., Fayolle, E. C., Romanzin, C., et al. 2013, *The Astrophysical Journal*, 779, 120
- Bertin, M., Romanzin, C., Doronin, M., et al. 2016, *The Astrophysical Journal*, 817, L12
- Carney, M. T., Hogerheijde, M. R., Guzmán, V. V., et al. 2019, 623, A124
- Carney, M. T., Hogerheijde, M. R., Loomis, R. A., et al. 2017, *Astronomy & Astrophysics*, 605, A21
- Cruz-Diaz, G. A., Martín-Doménech, R., Moreno, E., Muñoz Caro, G. M., & Chen, Y.-J. 2018, *Monthly Notices of the Royal Astronomical Society*, 474, 3080
- Cruz-Diaz, G. A., Martín-Doménech, R., Muñoz Caro, G. M., & Chen, Y.-J. 2016, *Astronomy & Astrophysics*, 592, A68
- Cruz-Diaz, G. A., Muñoz Caro, G. M., Chen, Y.-J., & Yih, T.-S. 2014, *Astronomy & Astrophysics*, 562, A119
- Dartois, E., Chabot, M., Id Barkach, T., et al. 2019, *Astronomy & Astrophysics*, 627, A55
- Dupuy, R., Bertin, M., Féraud, G., et al. 2017a, *Astronomy & Astrophysics*, 603, A61
- Dupuy, R., Féraud, G., Bertin, M., et al. 2017b, *Astronomy & Astrophysics*, 606, L9
- Esplugues, G. B., Cazaux, S., Meijerink, R., Spaans, M., & Caselli, P. 2016, *Astronomy & Astrophysics*, 591, A52
- Esplugues, G. B., Cazaux, S., Meijerink, R., Spaans, M., & Caselli, P. 2017, *Astronomy & Astrophysics*, 598, C1

- Fayolle, E. C., Bertin, M., Romanzin, C., et al. 2011, *The Astrophysical Journal*, 739, L36
- Féraud, G., Bertin, M., Romanzin, C., et al. 2019, *ACS Earth and Space Chemistry*, 3, 1135
- Fillion, J.-H., Fayolle, E. C., Michaut, X., et al. 2014, *Faraday Discussions*, 168, 533
- France, K., Schindhelm, E., Bergin, E. A., Roueff, E., & Abgrall, H. 2014, *The Astrophysical Journal*, 784, 127
- Gredel, R., Lepp, S., & Dalgarno, A. 1987, *The Astrophysical Journal*, 323, L137
- Guzmán, V., Pety, J., Goicoechea, J. R., Gerin, M., & Roueff, E. 2011, *Astronomy & Astrophysics*, 534, A49
- Guzmán, V. V., Goicoechea, J. R., Pety, J., et al. 2013, *Astronomy & Astrophysics*, 560, A73
- Heays, A. N., Bosman, A. D., & van Dishoeck, E. F. 2017, *Astronomy & Astrophysics*, 602, A105
- Le Petit, F., Nehme, C., Le Bourlot, J., & Roueff, E. 2006, *The Astrophysical Journal Supplement Series*, 164, 506
- Ligterink, N. F. W., Walsh, C., Bhuin, R. G., et al. 2018, *Astronomy & Astrophysics*, 612, A88
- Mathis, J. S., Mezger, P. G., & Panagia, N. 1983, *Astronomy & Astrophysics*, 128, 212
- Nahon, L., de Oliveira, N., Garcia, G. A., et al. 2012, *Journal of Synchrotron Radiation*, 19, 508
- Öberg, K. I., van Dishoeck, E. F., & Linnartz, H. 2009, *Astronomy and Astrophysics*, 496, 281
- Vastel, C., Ceccarelli, C., Lefloch, B., & Bachiller, R. 2014, *The Astrophysical Journal*, 795, L2
- Walsh, C., Loomis, R. A., Öberg, K. I., et al. 2016, *The Astrophysical Journal*, 823, L10
- Walsh, C., Millar, T. J., Nomura, H., et al. 2014, *Astronomy & Astrophysics*, 563, A33
- Walsh, C., Vissapragada, S., & McGee, H. 2017, *IAU*, 8